Testing the number of neutrino species with a global fit of neutrino data

Manuel Ettengruber,[1,2,*] Alan Zander,[3,†] and Philipp Eller[3,‡]
[1]*Arnold Sommerfeld Center, Ludwig-Maximilians-Universität, Theresienstraße 37, 80333 München, Germany*
[2]*Max-Planck-Institut für Physik, Föhringer Ring 6, 80805 München, Germany*
[3]*Technical University Munich (TUM), James-Franck-Strasse 1, 85748 Garching, Germany*

(Received 1 February 2024; accepted 18 April 2024; published 13 May 2024)

We present the first experimental constraints on models with many additional neutrino species with a similar Yukawa coupling with their right-handed partners among the additional Higgsed sectors by an analysis of current neutrino data. These types of models are motivated as a solution to the hierarchy problem by lowering the species scale of gravity to TeV. Additionally, they offer a natural mechanism to generate small neutrino masses and provide interesting dark matter candidates. This study analyzes data from DayaBay, KamLAND, MINOS, NOνA, and KATRIN. We do not find evidence for the presence of any additional neutrino species, therefore we report lower bounds on the allowed number of neutrino species realized in nature. For the normal/inverted neutrino mass ordering, we can give a lower bound on the number of neutrino species of $\mathcal{O}(30)$ and $\mathcal{O}(100)$, respectively, over a large range of the parameter space.

DOI: 10.1103/PhysRevD.109.095016

I. INTRODUCTION

Neutrino oscillations are so far the only phenomena of known particles that cannot be explained within the Standard Model (SM). The usual approach to explain them is by giving the neutrino a mass. Neutrino oscillation would then result from a mismatch between the flavor and the mass basis. Despite the success of this framework, several questions remain unanswered like the absolute value of neutrino masses and what mechanism generates them.

Of course, it could be the usual Higgs-Mechanism with a very small Yukawa coupling. But first, one could be puzzled about the smallness of the Yukawa coupling and second, the fact that the right-handed partner,ν_R, would be uncharged under the SM gauge group opens the gate for very different mechanisms that would be a candidate for mass generation for the neutrino. For example, could the neutrino be a Majorana particle which would mean that the mass term is generated by a higher dimensional operator with a large cutoff scale [1]. A very prominent mechanism that realizes this by introducing a heavy, right-handed, Majorana particle is the seesaw mechanism [2–6]. Because a high cutoff scale is introduced such solutions to the neutrino mass problem are called UV solutions.

An alternative to addressing the neutrino mass problem are IR solutions. For example, one possibility is the proposal that neutrinos acquire a mass resulting from the gravitational θ-term [7]. Another way offer theories in which the scale of gravity is lowered to TeV scale due to the presence of many additional light states, also called species [8,9], and these theories we want to investigate further in this work.

So far two models of this kind are known namely the Arkani-Hamed-Dimopoulos-Dvali (ADD) model [10,11], in which the light states are introduced by a Kaluza-Klein tower of gravitons, and the Dvali-Redi (DR) model with many copies of the SM [12]. How small neutrino masses can be realized in the ADD and DR model was shown in [13] and [12], respectively. Later it was demonstrated that ADD is a specific version of the many species approach [8] and afterward that small Dirac masses for neutrinos is an inherent feature of this kind of theories [14] even though they were originally introduced to solve the hierarchy problem. Additionally, these theories have built-in solutions to the dark matter problem [12,15,16]. Addressing this trinity of problems at the same time makes these theories candidates that are worth further investigation.

Let us stop here for a moment and see how these models fit into the bigger picture. The core motivation for these models comes from the following equation

$$M_f \leq \frac{M_P}{\sqrt{N_{sp}}}, \tag{1}$$

*manuel@mpp.mpg.de
†alan.zander@tum.de
‡philipp.eller@tum.de

where M_P is the Planck mass, M_f the fundamental scale of gravity and N_{sp} is the number of additional light states. This equation gives us a way to solve the hierarchy problem of particle physics [8,9] because if N_{sp} is a large number of order $\mathcal{O}(10^{32})$ the fundamental scale of gravity can be lowered down to TeV scale. This new scale M_f in the context of string theory is often called the "species scale" [17–20]. This scale, and not M_P as one would naively think, marks the moment when gravity becomes nonperturbative and the description of Einstein's gravity breaks down.

The fact that the separation of M_f from M_P influences the mass generation of the neutrino opens the exciting possibility to test the ADD and DR model with neutrino experiments that operate on energies far below the energy scale M_f [12,14,21]. In this paper, we want to do exactly that.

The ADD model was already the subject of previous research in [22–33] and we will therefore focus on the DR model that has not been tested experimentally so far. We want to use the characteristic pattern for neutrino oscillations that the DR model predicts and search for it in neutrino experiments namely KamLAND [34], DayaBay [35,36], MINOS/MINOS+ [37], NOνA [38], and KATRIN [39]. We perform a global fit based on the publicly available data coming from these experiments and search for the imprints of the DR model in the data. Complementary theoretical considerations rooted in the cosmological history of the universe have been undertaken in [40,41] and we compare our findings with these results. In this work, we focus on terrestrial experiments to be independent of model-dependent cosmological scenarios.

This paper is organized as follows: In Sec. II we will introduce what the DR model actually is and how neutrino oscillations arise in this model. Then we carry on by describing our analysis strategy for the above-mentioned experiments in Sec. III. Finally, we present our results in Sec. IV and give our conclusion and outlook in Sec. V.

II. NEUTRINO OSCILLATIONS WITH MANY ADDITIONAL LIGHT STATES

A particularly interesting case of theories with many additional species is the DR model where one introduces many SM copies that only interact gravitationally among each other [12]. Such a scenario of many dark SM sectors could be easily realized in an extra-dimensional framework where the additional sectors are localized on displaced branes in the bulk as described in [42]. In such a situation the right-handed neutrino of every copy ν_R can play a special role because it can form the following Dirac term with their left-handed counterparts

$$(HL)_i \lambda_{ij} \nu_{Rj} + \text{H.c.} \tag{2}$$

Here H, L is the Higgs-/Lepton- Doublet λ is a $N \times N$ Yukawa matrix, and the labels i, j denote the different SM-copies.

Because one introduces SM copies a full permutation symmetry among all neutrinos holds and this has the effect that the number of introduced parameters is very limited. These are: The number of neutrino copies N and the Yukawa-matrix whose allowed structure is set to

$$\lambda_{ij} = \begin{pmatrix} a & b & \dots & b \\ b & a & \dots & b \\ \vdots & \vdots & \ddots & \vdots \\ b & b & \dots & a \end{pmatrix}. \tag{3}$$

From unitarity, we get the following bound on b

$$b \leq \frac{1}{\sqrt{N}}, \tag{4}$$

and we expect a being of the same order because a and b are of the same nature. After diagonalizing the resulting mass matrix one gets the following expression for the neutrino made up of the mass eigenstates ν_1^m, ν_H^m

$$|\nu_1\rangle = \sqrt{\frac{N-1}{N}} |\nu_1^m\rangle + \frac{1}{\sqrt{N}} |\nu_H^m\rangle, \tag{5}$$

with the corresponding eigenvalues

$$m_1 = (a-b)v, \tag{6}$$

$$m_H = [a + (N-1)b]v, \tag{7}$$

where v is the vacuum expectation value of the Higgs. From (6) we see that due to the suppression of the Yukawa-couplings with $\frac{1}{\sqrt{N}}$ the mass experiences the same suppression. This gives us a different view to explain the smallness of the neutrino mass compared to the seesaw mechanism that offers a solution lying in the UV. Here the mass of the neutrino gets suppressed by the large number of additional light states. This gives us a solution to the neutrino mass problem that lies in the infrared (IR). This mechanism was originally described in [12] and in [14] the setup was generalized to a three-flavor case leading to the expression for example for an electron neutrino

$$\begin{aligned} |\nu_e\rangle = &\sqrt{\frac{N-1}{N}} (U_{e1} |\nu_1^m\rangle + U_{e2} |\nu_2^m\rangle + U_{e3} |\nu_3^m\rangle) \\ &+ \frac{1}{\sqrt{N}} (U_{e1} |\nu_H^{m_1}\rangle + U_{e2} |\nu_H^{m_2}\rangle + U_{e3} |\nu_H^{m_3}\rangle), \end{aligned} \tag{8}$$

and it was also shown, that by breaking the permutation symmetry among the copies by different vacuum expectation values, the masses of the heavy mass eigenstate [see (7)] can be decoupled from N. The result is that the masses for the light and the heavy mass eigenstates are related via

$$m_i^H = \mu m_i, \tag{9}$$

with μ being a factor that is the same for all three mass eigenstate pairs. This reduces the number of parameters beyond the SM down to just two parameters: N and μ.

This is a specific feature of the neutrino extension of the DR model because the SM flavor mixing happens within one copy and the mixing among copies happens within the species (see [14]). Under this assumption, the above situation arises without any further input. This makes this theory highly predictive and offers us a smoking gun signature by relating the additional mass eigenstates to the SM ones by just one additional parameter.

It is noteworthy that in this analysis the DR model serves as a benchmark for a class of theories that have a similar Yukawa coupling among the additional Higgsed sectors. Slight deviations from the Yukawa matrix of the form (3) would be too small to be resolved by the experiments. Also, we would like to comment on the fact that we are investigating only a Dirac operator in our model. In [14] also a Weinberg operator was investigated but both operators lead to the same phenomenology in our analysis. Moreover, the suppression scale of the Weinberg operator is already an explanation for small neutrino masses due to the Seesaw mechanism. This means from a conceptual point of view the introduction of an effective operator with an additional free parameter is unnecessary in our model because it offers already an alternative suppression mechanism.

From the expression (8) one can derive now the survival probability for such an electron neutrino with energy E in the following way

$$\begin{aligned} P(\nu_e \to \nu_e) = & \left(\frac{N-1}{N}\right)^2 \sum_{i=1}^{3}\sum_{j=1}^{3} |U_{ei}|^2 |U_{ej}|^2 e^{\frac{i(m_i^2-m_j^2)t}{2E}} \\ & + \frac{N-1}{N^2} \sum_{i=1}^{3}\sum_{j=4}^{6} |U_{ei}|^2 |U_{ej}|^2 e^{\frac{i(m_i^2-m_j^2)t}{2E}} \\ & + \frac{N-1}{N^2} \sum_{i=4}^{6}\sum_{j=1}^{3} |U_{ei}|^2 |U_{ej}|^2 e^{\frac{i(m_i^2-m_j^2)t}{2E}} \\ & + \frac{1}{N^2} \sum_{i=4}^{6}\sum_{j=4}^{6} |U_{ei}|^2 |U_{ej}|^2 e^{\frac{i(m_i^2-m_j^2)t}{2E}}. \end{aligned} \tag{10}$$

Example oscillation patterns of this formula for the choice of a few parameter values, assuming normal mass ordering (NO), are depicted in Figs. 1–3 in the L/E regimes of interest.

But not just the oscillator behavior of neutrinos get affected in this theory but the additional mass eigenstates will influence the effective mass of interacting neutrino states. This offers us another way to restrict the parameter space of the DR model by using the upper bound on the electron neutrino mass via the following formula

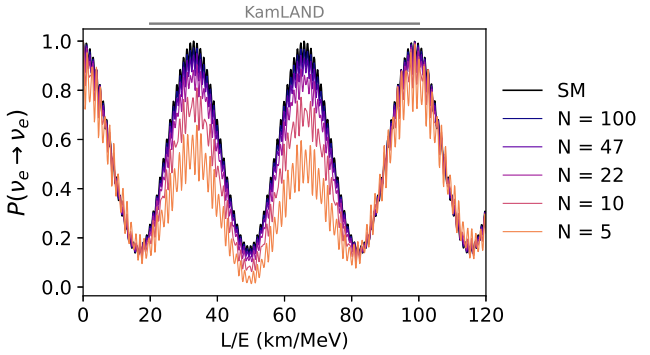

FIG. 1. Example electron neutrino survival probabilities at an L/E around the solar mass splitting for various numbers of extra species N and mass factor $\mu = 5$, assuming NO.

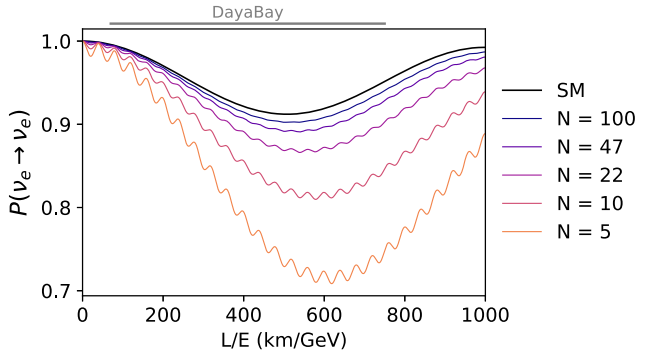

FIG. 2. Example electron neutrino survival probabilities at an L/E around the atmospheric mass splitting for various numbers of extra species N and mass factor $\mu = 5$, assuming NO.

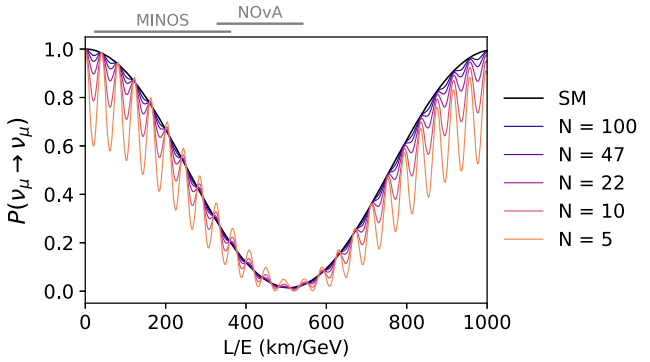

FIG. 3. Example muon neutrino survival probabilities at an L/E around the atmospheric mass splitting for various numbers of extra species N and mass factor $\mu = 5$, assuming NO.

$$\begin{aligned} m_{\nu_e}^2 = & \, m_{\text{lightest}}^2 \left(\frac{N+\mu^2-1}{N}\right) + \frac{N-1}{N}(\Delta m_{12}^2 U_{e2}^2 \\ & + \Delta m_{13}^2 U_{e3}^2) + \frac{\mu^2}{N}(\Delta m_{12}^2 U_{e2}^2 + \Delta m_{13}^2 U_{e3}^2). \end{aligned} \tag{11}$$

So we have two types of experiments to determine our DR parameters, neutrino oscillation experiments, and neutrino

mass detection experiments. In principle, one could also use data from neutrino mass sum probes coming from cosmology. But as we said, in this paper we want to restrict ourselves to experiments that are independent from the cosmological model.

The predictive power of the theory discussed above becomes evident when one compares it with a general ansatz where one sets the number of additional sterile neutrinos $n_s = 3$. In such an approach the number of independent physical mixing angles is $3(n_s + 1) = 12$ and Dirac phases are $2n_s + 1 = 7$. On top we have three additional masses for the sterile neutrinos, m_1^s, m_2^s, m_3^s [43]. The total number of independent parameters of a $3 + 3$ approach is 22. The DR model has two BSM parameters, N, and μ. Because μ relates the masses of the SM neutrinos with the sterile neutrinos, another parameter of interest is the mass of the lightest neutrino m_{lightest}. This gives us a number of 3 parameters that are of additional interest for neutrino oscillations on top of the usual SM parameters. The total number of parameters to fit neutrino oscillations is then 9. Obviously, the DR model offers a more minimal framework to perform a BSM neutrino fit than a general $3 + 3$ neutrino fit.

III. DATA ANALYSIS

Overall, our analysis has the following free parameters:

$$\{\delta_{CP}, \theta_{12}, \theta_{13}, \theta_{23}, \Delta m_{12}^2, \Delta m_{13}^2, m_{\text{lightest}}, N, \mu\}, \quad (12)$$

where $\delta_{CP}, \theta_{12}, \theta_{13}, \theta_{23}$ are the well-known parameters of the Pontecorvo–Maki–Nakagawa–Sakata (PMNS) matrix and $\Delta m_{12}^2, \Delta m_{13}^2$ the differences of the mass eigenstates.

To determine the values of these parameters we perform a combined maximum likelihood fit. Because we analyze neutrino data for the first time in the DR regime we do not have prior knowledge of the parameters shown in Eq. (12). Therefore, we have to perform an independent analysis of the available experimental data and cannot rely on previous SM global fits. Also, because every SM mixing angle experiences a correction by this model and the additional mass splittings can in principle take very different values our statistical analysis has to perform a fit for all 9 free parameters.

The answer to the question of which experiment to include in our analysis we based on the fact that the neutrino oscillation experiments measure different combinations of the fraction $\frac{L}{E}$, with L being the base lengths of the experiment and E the energies of the neutrinos. Including a variety of different experiments has two effects. First, we can choose for every SM parameter at least one experiment that restrains this parameter. Second, a broad range of the different experiments allows us also to search for deviations in SM oscillations coming from very small to quite large mass splittings between the SM mass eigenstates and the BSM ones.

Now let us discuss our specific choice of experiments and what we expect how the different experiments contribute to the resulting exclusion limits of the BSM parameters. We want to point out here again that the BSM contribution to neutrino experiments scales with $1/N$. This means that for larger values of N we expect less influence and not more. Exactly this behavior makes neutrino experiments particularly interesting to study because in usual high-energy experiments like LHC larger values of N lead to stronger effects. This makes both approaches complementary as one gives lower bounds on N and the other one gives upper bounds.

Maybe the intuitively easiest experiment to understand is KATRIN. The additional mass eigenstates will contribute to the effective mass of the electron neutrino and the model parameters controlling this mass are m_{lightest} and μ. Meanwhile, oscillations experiments are also sensitive to μ, KATRIN is the only experiment in our analysis that can restrain m_{lightest}. This is important because the masses of the SM states are uniquely determined after m_{lightest} is fixed and μ is then relating the SM masses to the BSM ones. Therefore, for large μ the BSM masses are higher and the electron neutrino mass gets stronger influenced. Due to this, we expect KATRIN to become most relevant in the regime where μ has large values.

The KamLAND experiment is necessary for our analysis because it restricts the SM parameters Δm_{12}^2 and θ_{12}. The expected sensitivity for BSM parameters we can estimate if we look at Fig. 1 where we see that the deviations from the SM oscillations become significant for $N \leq 10$.

DayaBay on the other hand is much more sensitive to N as we see from Fig. 2. Together with the fact that this experiment provides us with very high statistics in its data, we expect that DayaBay will contribute significantly to our final exclusion limit for the BSM parameters. Additionally it is restricting θ_{13} and Δm_{13}^2.

MINOS and NOνA are complementary. Because Noνa is located exactly at the oscillation maximum it provides very good sensitivity for SM parameters θ_{23} and Δm_{13}^2 but at the same time it is lacking sensitivity to the BSM parameters (see Fig. 3). Minos on the other hand is located off maximum which is suited for searching for BSM contributions to the oscillation pattern.

Putting the pieces together we can define the following likelihood

$$\mathcal{L}_{\text{comb}} = \mathcal{L}_{\text{KATRIN}} \times \mathcal{L}_{\text{MINOS}} \times \mathcal{L}_{\text{KamLAND}} \times \mathcal{L}_{\text{DayaBay}} \times \mathcal{L}_{\text{NO}\nu\text{A}}, \quad (13)$$

where we treated every dataset independently which allows us to construct $\mathcal{L}_{\text{comb}}$ as a product of all the single

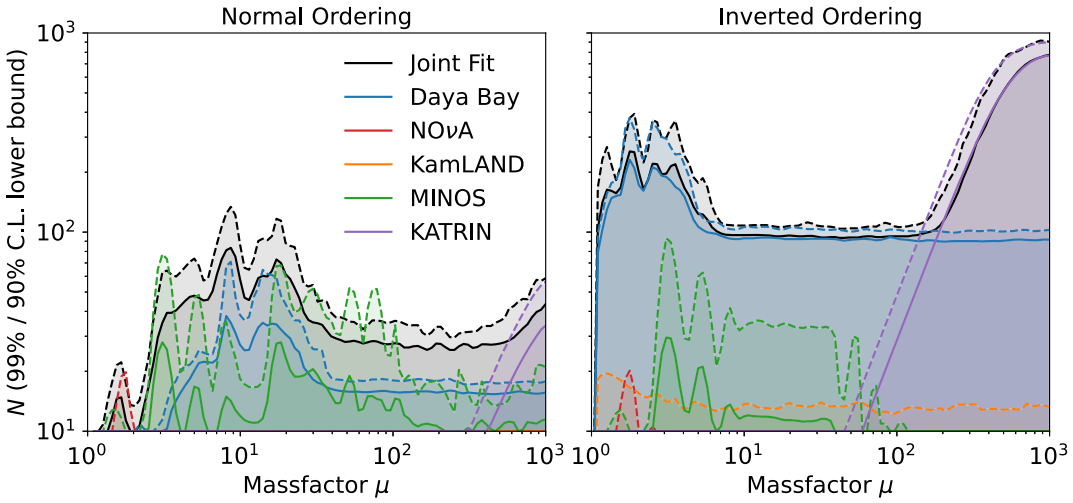

FIG. 4. Lower bounds on the number of species N as a function of the mass factor μ for the normal and inverted neutrino mass ordering, respectively. The solid and dashed lines denote the 90% and 99% asymptotic confidence levels (CL), the shaded areas are excluded. The colorful lines represent fits of individual datasets, and the black lines result from a combined fit of all four datasets.

likelihoods of the experiments. For our statistical analysis, we use a likelihood ratio test statistic. In case the alternate hypothesis (DR model) would be preferred over the null hypothesis (SM) with a significance greater than 3σ, we would investigate a signal. Otherwise, we would set exclusion limits on the parameter N as a function of μ, while profiling over all remaining parameters.

In this analysis, public data was used that was given in the papers [34–39]. For the MINOS and MINOS + analysis we use the far detector (FD) CC and NC data and In the Noνa analysis we use the muon disappearance data. For each experiment, a fit of the SM model was performed and compared with the findings of the articles. We did the comparison among the reported SM parameters as well in checking if our predicted oscillated neutrino spectrum aligns with the ones of the papers. When this was the case we carried on and checked if the fit of the DR model represents the data as well. Because in the high N limit the DR model contains the SM oscillation behavior we expect that the DR model will at least result in an equally good fit of the data as the SM. This meticulous comparison was essential to ensure the reliability and validity of the subsequent analysis employing the proposed DR model.

A deeper summary of how each experiment was analyzed is given in the Appendix.

IV. RESULTS

The best fitting DR hypothesis assuming normal ordering (NO) yields a value in log-likelihood units of 4.37 better than the standard model fit, while for the inverted ordering (IO) the difference equates to 2.49 log-likelihood units. These numbers, assuming Wilks' theorem and considering the three additional degrees of freedom $(N, \mu, m_{\text{lightest}})$, correspond to a significance of 1.8σ and 0.97σ, respectively, for the NO and IO case. Since neither of these are at a significance $>3\sigma$, we proceed to set exclusion limits.

The resulting limits are shown in Fig. 4 for NO and IO, respectively. First, we see that in the IO case, we can give a lower bound on $N > \mathcal{O}(10^2)$ quite consistently over the range of μ. The exclusion limit for $\mu < 10^2$ is set by the oscillations experiments, meanwhile for $\mu > 10^2$ the exclusion is basically dominated by KATRIN as expected. Because oscillations experiments measure the survival probability (10) these experiments test a beyond SM contribution that scales in the first order as $\frac{1}{N}$. This means that for $N > \mathcal{O}(10^2)$ the corrections coming from the DR model are of order $<1\%$ which is consistent with reported experimental measurements that have uncertainties around 1–5%. The situation is more complex in the NO case. We see in general that the bounds on N are weaker than in the IO case. The significance of KATRIN is reduced compared to the IO case and starts affecting the exclusion limit for $\mu > 300$. Nevertheless, for higher values of μ it shows a similar behavior as in the NO case but with a reduced sensitivity. In the parameter space where $\mu > 2$ one can give a rough bound on $N > 30$. If $\mu \leq 2$ then one can see that experiments start losing their sensitivity to this model because the mass-splitting for the BSM states becomes too small to be resolved by experiments.

In general our limits are to be interpreted for $N \geq 2$, since for $N = 1$ the SM case is recreated [see (8)]. Also, for $\mu = 1$ we get back to the SM since mixing becomes degenerate, and that is why limits become very weak when getting close to $\mu = 1$ as can be seen in either plots.

If we compare our numerical results with what we would have expected by the oscillograms as described in the

previous section we see that our expectations agree with our results.

V. CONCLUSION

In this work, we presented the first experimental test of additional neutrino species using experimental data. We concluded that depending on the mass hierarchy realized in nature we can set a lower limit on the number of neutrino species as $N > \mathcal{O}(30)$ for NO and $N > \mathcal{O}(100)$ for IO over a wide range of the parameter space.

Using the fact that the Dirac operator allows communication via the right-handed neutrino between the sectors one can also add cosmological considerations to give lower bounds on the number of neutrino species [41]. Compared to these bounds the bounds resulting from experiments are weaker but more robust due to the fact that our results do not depend on the cosmological history beyond BBN.

Therefore our results show, that neutrino experiments are especially suited for testing models with additional neutrino species because compared to other physics we can give a lower bound on N meanwhile LHC [8,9] and axion physics [40] give an upper bound on the number of species.

The complementary nature of neutrino experiments operating in the IR to UV experiments is quite exciting and future experiments like JUNO [44] and DUNE [45] are designed to improve our knowledge about the lepton mixing parameters by one order of magnitude which will give us the possibility to close the open window of the parameter space even further.

Together with theoretical considerations [40,41], UV and IR experiments can help us to restrict the possible range of N_{sp} and reveal where we could expect the true scale of Quantum Gravity.

ACKNOWLEDGMENTS

We are thankful for our discussions with Allen Caldwell and Gia Dvali. This work has been supported by the Deutsche Forschungsgemeinschaft (DFG, German Research Foundation) under the Sonderforschungsbereich (Collaborative Research Center) SFB1258 "Neutrinos and Dark Matter in Astro- and Particle Physics."

APPENDIX

In the appendix, we describe in more detail how the datasets from the different experiments have been analyzed for our reinterpretation.

A. DayaBay

DayaBay was a reactor neutrino experiment located in China to measure the parameters θ_{13} and Δm^2_{32}. Together with [35] the collaboration released their dataset of 26 data points which we analyzed in this work. Because DayaBay's neutrino flux is sourced by several nuclear reactors which have different baselengths to the experimental halls the detectors are placed in, we calculated the contribution of every reactor to the overall flux at the experimental site. DayaBay consists of experimental halls close to the reactor to determine the predicted flux in the far experimental hall. The data of the far experimental hall (EH3) was used in this analysis. The geometric averaged baseline to EH3 is around 1663 m. In order to incorporate the systematical uncertainties of the experiment we took the covariance matrix published in [36] and scaled the general covariance matrix accordingly to the data which is analyzed here. Performing a fit for standard mixing parameters, our results are shown in Fig. 5, including a goodness-of-fit p-value calculated via χ^2 with degrees of freedom equal to the number of data points. The resulting mixing parameters of our analysis are well consistent with those reported by the collaboration. DayaBay official results are $\sin^2 2\theta_{13} = 0.0856 \pm 0.0029$, $\Delta m^2_{32} = 2.471^{+0.068}_{-0.070} \times 10^{-3}$ eV^2, while we extracted $\sin^2 2\theta_{13} = 0.0851 \pm 0.0022$ and $\Delta m^2_{32} = 2.45 \pm 0.065 \times 10^{-3}$ eV^2. Our fit returned a p-value of 0.51, which indicates a good agreement between the expected and observed spectra.

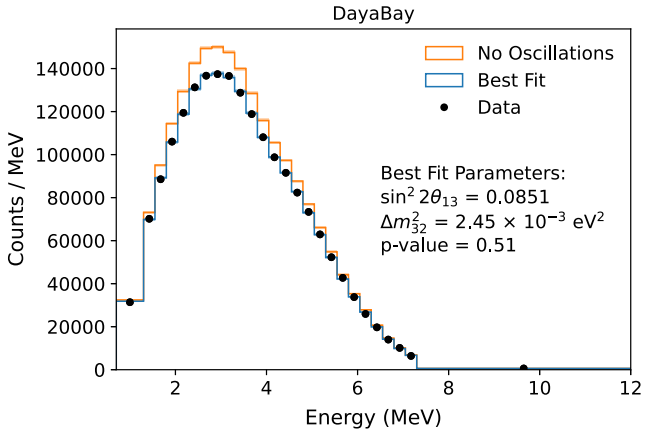

FIG. 5. The DayaBay energy spectrum of the counted neutrinos for the data (black), in case of no oscillations (orange), and our best fit (blue) in the case for NO. The shaded regions (invisible) are the total uncertainties.

B. KamLAND

KamLAND was a reactor experiment based in Japan designed to measure θ_{12} and Δm^2_{12}. We averaged the survival probability of the neutrino flux over all baselines of the reactors placed in Japan while neglecting the contribution from South Korea which is around 5% and the world contribution which is around 1%. Our analysis is based on the publication [34] that also includes a non-oscillated spectrum of the neutrino flux at the experiment. The necessary information was extracted from Fig. 1 in this publication. Due to lacking public information, we could not include a full covariance matrix and resorted to using a

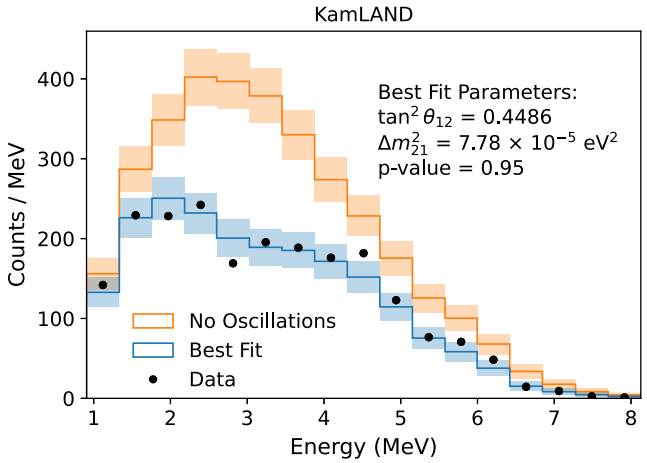

FIG. 6. The KamLAND energy spectrum of the counted neutrinos for the data (black), in case of no oscillations (orange), and our best fit (blue) in the case for NO. The shaded regions are the total uncertainties.

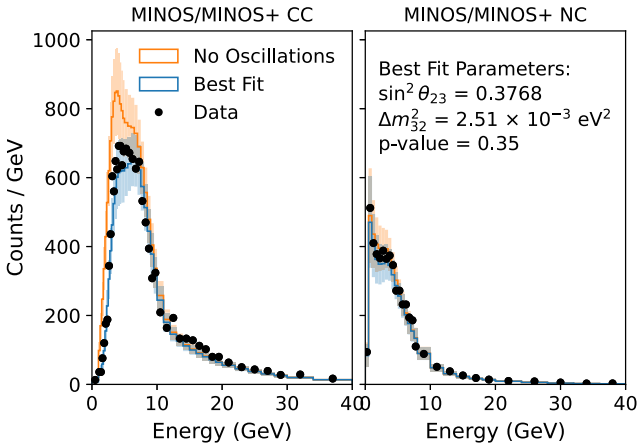

FIG. 7. The MINOS energy spectrum of the counted neutrinos for the data (black), in case of no oscillations (orange), and our best fit (blue) in the case for NO. The shaded regions are the total uncertainties.

diagonal covariance matrix which we constructed by using the uncertainties of the measured events per bin. In our final analysis, we incorporated 17 data points. The energy resolution was approximated by the bin width. Our fit results can be seen in Fig. 6 and compared with the official analysis results of $\tan^2\theta_{12} = 0.436^{+0.102}_{-0.081}$, $\Delta m^2_{21} = 7.49 \pm 0.20 \times 10^{-5}$ eV^2, ours are compatible with $\tan^2\theta_{12} = 0.4486 \pm 0.082$, $\Delta m^2_{21} = 7.78 \pm 0.29 \times 10^{-5}$ eV^2. The p-value of 0.95 in our analysis indicates a very good agreement of our model with the data.

C. MINOS

MINOS was an accelerator muon neutrino experiment located at Fermilab in the U.S. that operates slightly off maximum of the atmospheric mass splitting regime (see Fig. 3). In principle, it can be used to determine θ_{23} and Δm^2_{13} even though due to the energy range it is not optimal, but provides excellent data for searching for BSM signals in the oscillation pattern. This makes this experiment of particular interest for our analysis. We use the far detector (FD) CC and NC data from MINOS and MINOS+. The simulation templates, smearing matrices, covariance matrices, as well as the observed counts are provided in the data release accompanying the publication [37]. We implement our analysis by replicating the provided reference implementation. Our fit results are shown in Fig. 7 and are a good representation of the data. A SM analysis of this data was provided in [46] with $|\Delta m^2_{32}| = [2.28, 2.46] \times 10^{-3}$ eV^2 (68%), $\sin^2\theta_{23} = 0.35$–0.65 (90%), while our analysis indicated $|\Delta m^2_{32}| = [2.40, 2.65] \times 10^{-3}$ eV^2 (68%), $\sin^2\theta_{23} = 0.32$–0.69 (90%), which is consistent while slightly more conservative. Our p-value of 0.35 is very reasonable.

D. NOνA

Also, NOνA uses the same muon neutrino beam as MINOS but this experiment is located off-axis, resulting in maximum mixing if the atmospheric mass splitting regime (see Fig. 3). Therefore, it is optimized to restrict the SM parameters θ_{23} and Δm^2_{13}. We use the muon disappearance data from [47]. Forward and reversed horn current data is included in our analysis. A detector response is implemented via a smearing function defined according to the resolution specified in Table 2 in [47]. Our fit is shown in Fig. 8, the 68% confidence intervals of the official NOνA results are $\Delta m_{32} = [2.37, 2.52] \times 10^{-3}$ eV^2 and $\sin^2\theta_{23} = [0.52, 0.60]$, while we compute $\Delta m_{32} = [2.36, 2.49] \times 10^{-3}$ eV^2 and $\sin^2\theta_{23} = [0.56, 0.61]$. The p-value of 0.74 indicates good agreement between simulation and data.

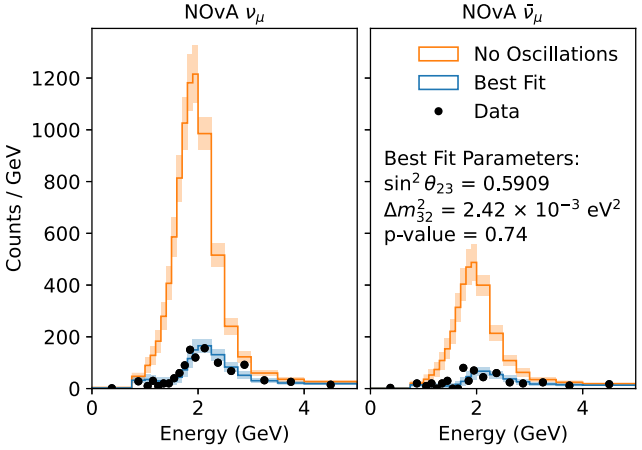

FIG. 8. The NOνA energy spectrum of the counted neutrinos for the data (black), in case of no oscillations (orange), and our best fit (blue) in the case for NO. The shaded regions are the total uncertainties.

E. KATRIN

Another relevant type of experiment is the direct measurement of the neutrino mass. The leading experiment for this is KATRIN which analyzes the spectrum of beta decays. In [39] the collaboration also performed a Bayesian analysis and reported a posterior on the mass of the electron neutrino. Because a flat prior on the m_{lightest} was used to calculate this result, we can easily interpret this posterior as our likelihood. We approximated the posterior distribution with a truncated normal distribution and calculated the predicted neutrino mass of the DR model with (11). In this analysis, we just evaluated the likelihood as described above and did not take into account the change in the shape of the energy distribution which would be caused by additional mass states in the expression for the flavor states. This is usually done in sterile neutrino searches with KATRIN and could still be improved in our analysis.

[1] S. Weinberg, Baryon and lepton nonconserving processes, Phys. Rev. Lett. **43**, 1566 (1979).
[2] P. Minkowski, $\mu \to e\gamma$ at a rate of one out of 10^9 muon decays?, Phys. Lett. **67B**, 421 (1977).
[3] M. Gell-Mann, P. Ramond, and R. Slansky, Complex spinors and unified theories, Conf. Proc. C **790927**, 315 (1979).
[4] T. Yanagida, Horizontal symmetry and masses of neutrinos, Prog. Theor. Phys. **64**, 1103 (1980).
[5] R. N. Mohapatra and G. Senjanovic, Neutrino mass and spontaneous parity nonconservation, Phys. Rev. Lett. **44**, 912 (1980).
[6] R. N. Mohapatra, Seesaw mechanism and its implications, in *Proceedings of the SEESAW25: International Conference on the Seesaw Mechanism and the Neutrino Mass* (2004), pp. 29–44, arXiv:hep-ph/0412379.
[7] G. Dvali and L. Funcke, Small neutrino masses from gravitational θ-term, Phys. Rev. D **93**, 113002 (2016).
[8] G. Dvali, Black holes and large N species solution to the hierarchy problem, Fortschr. Phys. **58**, 528 (2010).
[9] G. Dvali and M. Redi, Black hole bound on the number of species and quantum gravity at LHC, Phys. Rev. D **77**, 045027 (2008).
[10] N. Arkani-Hamed, S. Dimopoulos, and G. R. Dvali, The hierarchy problem and new dimensions at a millimeter, Phys. Lett. B **429**, 263 (1998).
[11] N. Arkani-Hamed, S. Dimopoulos, and G. R. Dvali, Phenomenology, astrophysics and cosmology of theories with submillimeter dimensions and TeV scale quantum gravity, Phys. Rev. D **59**, 086004 (1999).
[12] G. Dvali and M. Redi, Phenomenology of 10^{32} dark sectors, Phys. Rev. D **80**, 055001 (2009).
[13] N. Arkani-Hamed, S. Dimopoulos, G. R. Dvali, and J. March-Russell, Neutrino masses from large extra dimensions, Phys. Rev. D **65**, 024032 (2001).
[14] M. Ettengruber, Neutrino physics in TeV scale gravity theories, Phys. Rev. D **106**, 055028 (2022).
[15] N. Arkani-Hamed, S. Dimopoulos, G. R. Dvali, and N. Kaloper, Many fold universe, J. High Energy Phys. 12 (2000) 010.
[16] G. Dvali, I. Sawicki, and A. Vikman, Dark matter via many copies of the standard model, J. Cosmol. Astropart. Phys. 08 (2009) 009.
[17] G. Dvali and C. Gomez, Quantum information and gravity cutoff in theories with species, Phys. Lett. B **674**, 303 (2009).
[18] G. Dvali and D. Lust, Evaporation of microscopic black holes in string theory and the bound on species, Fortschr. Phys. **58**, 505 (2010).
[19] G. Dvali and C. Gomez, Species and strings, arXiv:1004.3744.
[20] G. Dvali, C. Gomez, and D. Lust, Black hole quantum mechanics in the presence of species, Fortschr. Phys. **61**, 768 (2013).
[21] G. R. Dvali and A. Y. Smirnov, Probing large extra dimensions with neutrinos, Nucl. Phys. **563B**, 63 (1999).
[22] P. A. N. Machado, H. Nunokawa, and R. Zukanovich Funchal, Testing for large extra dimensions with neutrino oscillations, Phys. Rev. D **84**, 013003 (2011).
[23] P. A. N. Machado, H. Nunokawa, F. A. P. dos Santos, and R. Z. Funchal, Bulk neutrinos as an alternative cause of the gallium and reactor anti-neutrino anomalies, Phys. Rev. D **85**, 073012 (2012).
[24] V. S. Basto-Gonzalez, A. Esmaili, and O. L. G. Peres, Kinematical test of large extra dimension in beta decay experiments, Phys. Lett. B **718**, 1020 (2013).
[25] I. Girardi and D. Meloni, Constraining new physics scenarios in neutrino oscillations from Daya Bay data, Phys. Rev. D **90**, 073011 (2014).
[26] W. Rodejohann and H. Zhang, Signatures of extra dimensional sterile neutrinos, Phys. Lett. B **737**, 81 (2014).
[27] J. M. Berryman, A. de Gouvêa, K. J. Kelly, O. L. G. Peres, and Z. Tabrizi, Large, extra dimensions at the deep underground neutrino experiment, Phys. Rev. D **94**, 033006 (2016).
[28] M. Carena, Y.-Y. Li, C. S. Machado, P. A. N. Machado, and C. E. M. Wagner, Neutrinos in large extra dimensions and short-baseline ν_e appearance, Phys. Rev. D **96**, 095014 (2017).
[29] G. V. Stenico, D. V. Forero, and O. L. G. Peres, A short travel for neutrinos in large extra dimensions, J. High Energy Phys. 11 (2018) 155.
[30] C. A. Argüelles *et al.*, New opportunities at the next-generation neutrino experiments I: BSM neutrino physics and dark matter, Rep. Prog. Phys. **83**, 124201 (2020).

[31] B. Abi *et al.* (DUNE Collaboration), Prospects for beyond the standard model physics searches at the Deep Underground Neutrino Experiment, Eur. Phys. J. C **81**, 322 (2021).
[32] V. S. Basto-Gonzalez, D. V. Forero, C. Giunti, A. A. Quiroga, and C. A. Ternes, Short-baseline oscillation scenarios at JUNO and TAO, Phys. Rev. D **105**, 075023 (2022).
[33] C. A. Argüelles *et al.*, Snowmass white paper: Beyond the standard model effects on neutrino flavor, Eur. Phys. J. C **83**, 15 (2023).
[34] A. Gando *et al.* (KamLAND Collaboration), Constraints on θ_{13} from a three-flavor oscillation analysis of reactor antineutrinos at KamLAND, Phys. Rev. D **83**, 052002 (2011).
[35] D. Adey *et al.* (Daya Bay Collaboration), Measurement of the electron antineutrino oscillation with 1958 days of operation at Daya Bay, Phys. Rev. Lett. **121**, 241805 (2018).
[36] F. P. An *et al.* (Daya Bay Collaboration), Improved measurement of the reactor antineutrino flux and spectrum at Daya Bay, Chin. Phys. C **41**, 013002 (2017).
[37] P. Adamson *et al.* (MINOS+ Collaboration), Search for sterile neutrinos in MINOS and MINOS + using a two-detector fit, Phys. Rev. Lett. **122**, 091803 (2019).
[38] M. A. Acero *et al.* (NOvA Collaboration), New constraints on oscillation parameters from ν_e appearance and ν_μ disappearance in the NOvA experiment, Phys. Rev. D **98**, 032012 (2018).
[39] M. Aker *et al.* (KATRIN Collaboration), Direct neutrino-mass measurement with sub-electronvolt sensitivity, Nat. Phys. **18**, 160 (2022).
[40] M. Ettengruber and E. Koutsangelas, Consequences of multiple axions in theories with dark Yang-Mills groups, arXiv:2307.10298.
[41] A. Zander, M. Ettengruber, and P. Eller, How many dark neutrino sectors does cosmology allow?, Eur. Phys. J. C **84**, 331 (2024).
[42] N. Arkani-Hamed, T. Cohen, R. T. D'Agnolo, A. Hook, H. D. Kim, and D. Pinner, Solving the hierarchy problem at reheating with a large number of degrees of freedom, Phys. Rev. Lett. **117**, 251801 (2016).
[43] J. Barry, W. Rodejohann, and H. Zhang, Light sterile neutrinos: Models and phenomenology, J. High Energy Phys. 07 (2011) 091.
[44] Z. Djurcic *et al.* (JUNO Collaboration), JUNO conceptual design report, arXiv:1508.07166.
[45] B. Abi *et al.* (DUNE Collaboration), Deep Underground Neutrino Experiment (DUNE), far detector technical design report, volume I introduction to DUNE, J. Instrum. **15**, T08008 (2020).
[46] L. H. Whitehead (MINOS Collaboration), Neutrino oscillations with MINOS and MINOS+, Nucl. Phys. **908B**, 130 (2016).
[47] M. A. Acero *et al.* (NOvA Collaboration), Improved measurement of neutrino oscillation parameters by the NOvA experiment, Phys. Rev. D **106**, 032004 (2022).